PHYSICO-CHEMICAL CONDITIONS IN GALACTIC INFRA-RED DARK CLOUDS

D. Teyssier, ESAC, PO Box 78, 28691 Madrid, Spain
M. Pérault, P. Hennebelle, LERMA, 24 rue Lhomond, 75005 Madrid

Introduction

Galactic Infra-Red Dark Clouds (IRDCs) have been evidenced more than a decade ago, both by the ISO (Pérault et al. 1996) and the MSX (Egan et al. 1998) missions. These structures appeared as dark patches seen on the mid-IR background, and more than 2000 objects were initially catalogued from the MSX survey. The first follow-ups at mm and submm wavelengths (Carey et al. 1998, 2000, Teyssier et al. 2002) have confirmed that these objects are dense and cold parts of GMCs. In the meantime, the cloud population was also shown to be present in the Outer Galaxy (Frieswijk et al., this conference). Recently, several studies based of Spitzer and high-resolution mm data (e.g. Beuther et al. 2007, Rathborne et al. 2007) have revealed the presence of embedded sources in massive gas core, likely progenitors of future massive stars.

We present here a detailed analysis of the physico-chemical conditions at work in the ISOGAL cloud sample introduced in Teyssier et al. 2002.

Temperatures

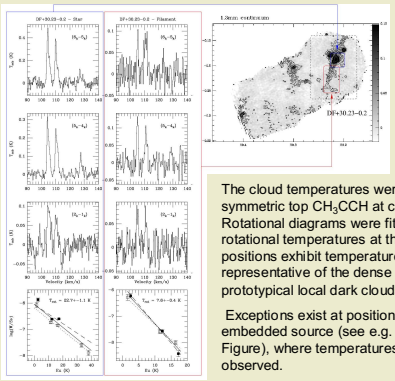

The cloud temperatures were estimated using the symmetric top CH_3CCH at cm and mm wavelengths. Rotational diagrams were fitted, allowing to infer rotational temperatures at the probed positions. Most positions exhibit temperatures in the range 5-10 K, representative of the dense cores observed in the prototypical local dark clouds (e.g. TMC-1, L134N).

Exceptions exist at positions showing evidence of embedded source (see e.g. the *Star* position in the left Figure), where temperatures in excess of 20 K are observed.

Left: Spectra of the (6_k-5_k), (5_k-4_k) and (2_k-1_k) transitions of CH_3CCH, as well as the resulting rotational diagrams, for 2 positions of the DF+30.23-0.20 cloud. Right: finding chart of the DF+30.23-0.20 cloud on a 1.2mm continuum map obtained at the IRAM 30-m.

Masses

We estimated the could masses following two approaches. The first is based on the inferred densities applied to an homogenous sphere of diameter equivalent to the cloud apparent size: M_{LVG}. The second is based on the virial mass: M_{vir}. The ratio $R = M_{vir}/M_{LVG}$ of these two masses can be used to study the gravitational stability of the clouds. Despite of the important error bars applying to the masses, this ratio is fairly constant among the sample, but behaviours differ depending on the molecule probed:

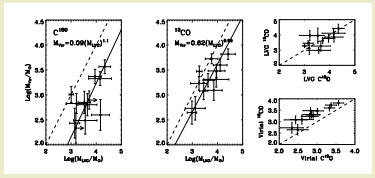

- For ^{13}CO, R = 0.62±0.4 is not incompatible with clouds in virial equilibrium
- For $C^{18}O$, R ~ 1/10, indicative of collapse, leading to active stellar formation (e.g. Yonekura et al. 1999)
- However, only few clouds are associated with YSOs
- Magnetic fields required to support against the collapse would be of the order of some mG, which is a lot !

Left and middle: virial masses versus LVG masses for $C^{18}O$ and ^{13}CO respectively. Exponential fit laws are also indicated. Right: comparison of respective LVG and virial masses for the two molecules.

Kinematic

Position-velocity diagrams have been prepared along dedicated cuts across the molecular emission of some of the clouds. They show changes in the velocity gradient signs, in some cases several times along the cut. Similar effects are seen in close-by clouds, where the nodes of these gradient changes coincide with the position of dark cores, where star formation could be triggered (e.g. Hily-Blant et al. 2005). Although the spatial scales are quite larger here, this could indicate that similar processes of star formation could be at work in the densest spots of the IRDCs.

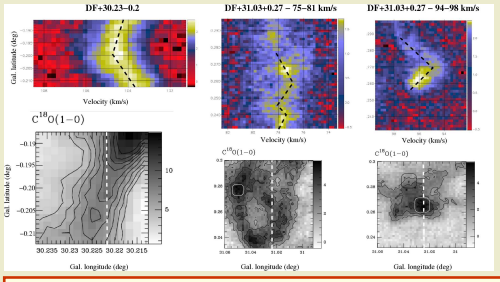

Position-velocity diagrams for three cuts across the $C^{18}O$(1-0) emission of IRDCs. The dashed black lines (added manually to the maps) indicate the changes in velocity signs along the cuts. The lower plots indicate the position of the cut on the integrated emission maps.

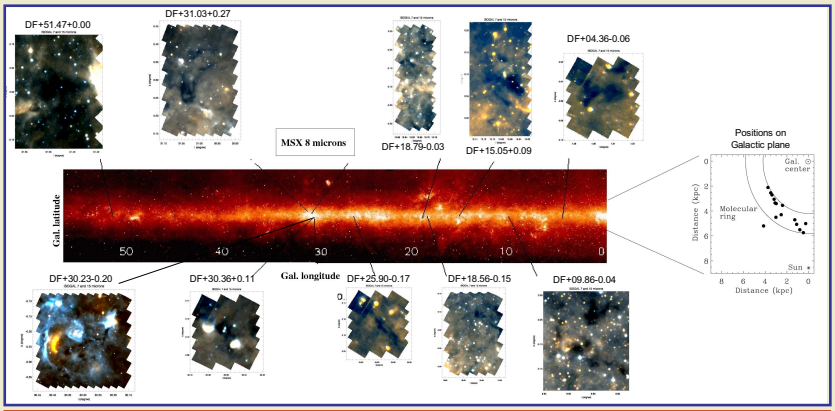

Left: Position of a sample of the IRDCs on the Galactic plan as covered by MSX (8 µm). Thumbnails show the composite images of the ISOGAL coverages at 7 and 15 microns. Right: location of the cloud sub-set projected over the Galactic plan

Density

The density analysis was conducted using multi-transition LVG simulations of the ^{13}CO, $C^{18}O$ and HC_3N dataset collected in a handful of lines. Kinetic temperatures were taken as the rotational temperature derived from CH_3CCH. The molecules considered here are found at different cloud depths along the line of sight and thus trace the densities in different layers of the objects. The figure below illustrates the best fit to HC_3N for some of the positions probed. The inferred HC_3N densities are found in excess of 10^5 cm^{-3}, while calculations based on the CO isotopes reveal numbers lower by one to two orders of magnitude.

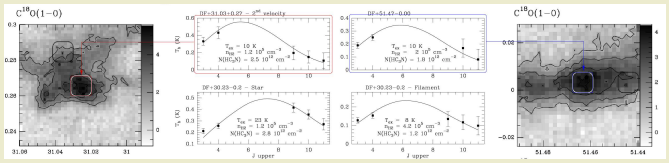

Middle: line intensities of HC_3N transitions for 4 of the studied clouds, with best LVG fit to the data and the corresponding parameters, assuming excitation temperatures derived from the rotational diagrams (see *Temperature* frame). Left and Right: $C^{18}O$(1-0) integrated intensity maps indicating the probed positions for DF+31.01+0.27 and DF+51.47-0.00. Positions for the DF+30.23-0.2 are the ones one the *Temperature* frame.

Depletion

Comparison of the integrated intensity of $C^{18}O$ with the visual extinction has often been used as a diagnostic of molecular depletion: as one penetrates towards the innermost layers of the cloud, the $C^{18}O$ emission stops to scale linearly with A_V and a recognizable break is observed (e.g. Alves et al. 1999). This effect is observed over all the clouds studied in the present sample. It was however noted that $C^{18}O$ may not be optically thin in the densest zones of these cloud cores. To confirm that the observed phenomenon could be invoked, even at the large scale (1 pc) implied in the present objects, we have done the following complementary studies:

$C^{17}O$ *vs* $C^{18}O$

- the optical thickness of $C^{18}O$ was checked against a thinner isotopomer: $C^{17}O$.
- both emission are well correlated, an in a ratio of order ~3.5, consistent with opacities below 1.
- this suggests that the break in the $C^{18}O$ *vs* A_V diagram is not due to radiative effects

N_2H^+ *vs* A_V

- the integrated emission of N_2H^+, a low sticking coefficient molecule, was compared to A_V.
- N_2H^+ emission correlated very well with the 1.2mm continuum and peaks where $C^{18}O$ has already flattened.
- N_2H^+ is almost inexistent up to A_V~10, but then rises, as its main destructor, $C^{18}O$, has likely started to deplete onto grains

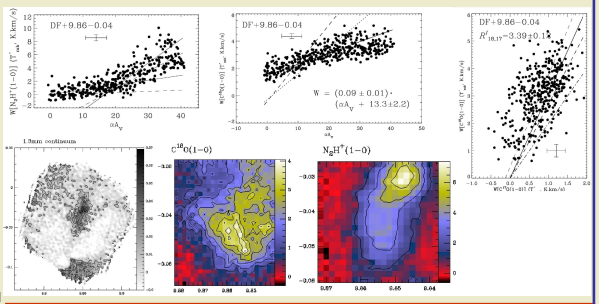

Up: scatter diagrams of N_2H^+ (1-0)and $C^{18}O$ (1-0) integrated intensity versus Av, and of the $C^{18}O$ (1-0) versus $C^{17}O$ (1-0) integrated intensities for the DF+09.86-0.04 cloud. Bottom: IRAM 30-m coverage of the 1.3mm continuum (mJy/11" beam), $C^{18}O$(1-0) and N_2H^+(1-0) respective integrated intensities (K.km/s).

References

Alves J. et al., 1999, ApJ 515, 265
Beuther H. et al., 2007, ApJ 656, L85
Carey S.J. et al., 1998, ApJ 508, 721
Carey S.J. et al., 2000, ApJ 542, L157
Egan M.P. et al., 1998, ApJ 494, L199
Frieswijk W. et al., 2007, A&A in press
Hily-Blant P. et al., 2005, A&A 440, 909
Pérault M. et al., 1996, A&A 315, L165
Rathborne et al., 2007, ApJ 662, 1082
Teyssier D. et al., 2002, A&A 382, 624
Yonekura et al., 1999, PASJ 51, 837